Tunnelling and Underground Space Technology 130 (2022) 104762

Contents lists available at ScienceDirect

Tunnelling and Underground Space Technology incorporating Trenchless Technology Research

journal homepage: www.elsevier.com/locate/tust

# Analysis of water ingress, grouting effort, and pore pressure reduction caused by hard rock tunnels in the Oslo region

Jenny Langford [a,*], Kristin H. Holmøy [b], Tom Frode Hansen [a], Karl Gunnar Holter [a], Eivind Stein [a]

[a] Norwegian Geotechnical Institute, Norway
[b] Norwegian University of Science and Technology, Norway

ARTICLE INFO

*Keywords:*
Urban tunnelling
Water ingress
Pore pressure
Settlements

ABSTRACT

Many subsurface projects in Scandinavia face challenges with settlement risk from water ingress into tunnels, due to challenging ground conditions featuring hard bedrock underlying soft, marine clay deposits. Pore pressure reduction in these clay-filled depressions can cause damage to nearby buildings and is one of the main risks associated with infrastructure development in Oslo. This paper presents an extensive database from 44 tunnels in the Oslo region, constructed between 1975 and 2020. The data consists of measured water ingress after pre-excavation grouting, reduction in pore pressure, pre-excavation grouting effort, and geological parameters. The data is analysed to identify trends and relations between key parameters, such as expected pore pressure reduction for a given water ingress rate and necessary grouting effort to obtain a given hydraulic conductivity of the grouted zone. The analysis shows that it is necessary to focus on pore pressure monitoring in future projects, rather than water ingress, to reduce the risk of unacceptable pore pressure reduction. Suggestions are given on how to optimise monitoring and follow-up of pre-excavation grouting to ensure that required watertightness is met.

## 1. Introduction

Tunnelling in urban areas is increasingly common, especially in connection with infrastructure development. Water ingress to bedrock tunnels can cause pore pressure reduction and consolidation settlements of soft soil deposits (Yoo, 2005; Yoo et al., 2012), leading to risk of damage to overlying buildings and infrastructure. The problem is illustrated in Fig. 1, showing water ingress to a bedrock tunnel, causing pore pressure reduction in a water bearing layer of sand and gravel at the bedrock surface, $\Delta u_F$. With time pore pressures, u, in the clay layer are affected, resulting in settlements. Fig. 2 shows expected settlements corresponding with a given pore pressure reduction at bedrock level, and clay thickness, for a normally consolidated deposit. Extensive pre-excavation grouting (PEG) is often necessary to reduce the water ingress and limit pore pressure reduction in urban areas.

In Oslo, Norway, the first documented case of settlements caused by pore pressure reduction during tunnelling was the construction of the first subway tunnel, Holmenkollbanen in 1912–1916. This project caused settlements up to 30–40 cm and extensive damage to apartments and office buildings above the tunnel, as far as 500 m away from the tunnel (Holmsen, 1953). Another well-known example, is the excavation of the Romeriksporten railway tunnel in the 1990s. The excavation of this tunnel caused major pore pressure reduction, resulting in up to 30 cm of differential settlement and extensive damage to at least 150 houses (Beitnes, 2002, Myrabø and Moss-Iversen, 2014).

Settlement damage caused by groundwater drawdown is a worldwide known problem in regions with soft soil ground conditions, with extreme consequences for society. The mechanism of ground settlements due to groundwater drawdown is well documented from excess pumping of groundwater from confined and layered aquifers, for example in Jakarta (Abidin et al., 2011), China (Xue et al., 2005, Zhu et al., 2015), Bangkok (Pien-wej et al., 2006), Mexico City (Ortega-Guerrero et al., 1999), Ca Mau Province, Vietnam (Karlsrud and Vangelsten, 2017), and Las Vegas (Burbey, 2002). However, fewer case studies on the settlements due to tunnelling induced groundwater drawdown have been reported. Severe settlements have been recorded due to underground construction in Hong Kong (Garshol et al., 2012; Garshol et al., 2014) and Shanghai (Shen et al., 2014), China, Seoul, South Korea (Yoo et al., 2012), and São Paulo, Brazil (Barton and Quadros, 2019). These case studies all highlight the importance of groundwater control and need for PEG.

As a result of the problems during construction of the

* Corresponding author at: Postboks 3930 Ullevål stadion, 0806 OSLO, Norway.
*E-mail address:* jenny.langford@ngi.no (J. Langford).

https://doi.org/10.1016/j.tust.2022.104762
Received 30 December 2021; Received in revised form 2 September 2022; Accepted 18 September 2022
Available online 28 September 2022

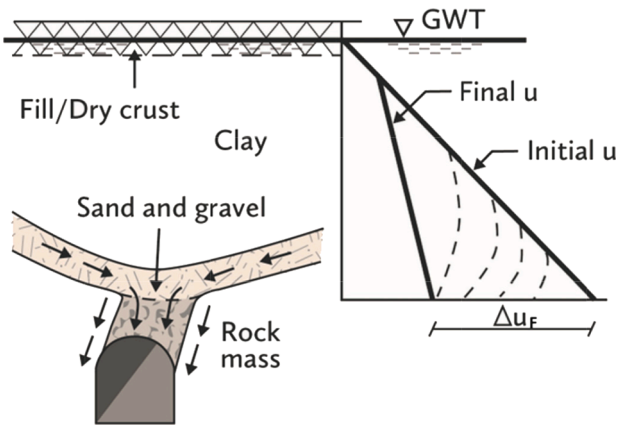


**Fig. 1.** Illustration of water ingress to a bedrock tunnel causing pore pressure reduction in a water bearing layer over the bedrock (revised from Karlsrud et al., 2003).

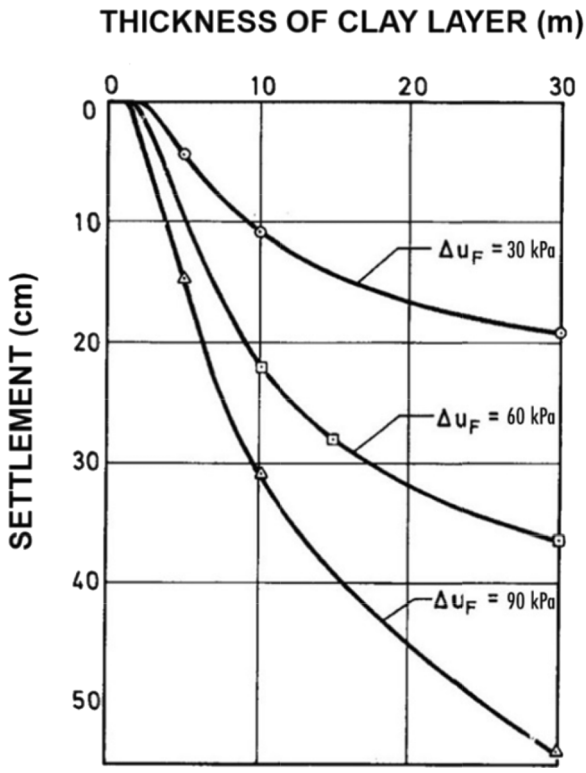


**Fig. 2.** Consolidation settlements caused by pore pressure reduction (revised from Karlsrud et al., 2003).

Romeriksporten tunnel, the Norwegian tunnelling industry initiated a comprehensive research project to better understand the effects of tunnelling on the surrounding environment (Lindstrøm & Kveen, 2005, NTS, 1995, NTS, 2001). As part of this project, Karlsrud et al. (2003) summarized construction and monitoring data for tunnels completed between 1975 and 2002, including grouting efforts (both drilling and grout consumption), water ingress measurements and pore pressure reduction measured at the bedrock surface.

Since the 1980s it has been standard practice to use cement-based PEG applying high pumping pressures (above 50 bar) in Norway, except for limited use of chemical grouts, mainly for post-excavation grouting. After the events of the Romeriksporten tunnel, limits on water ingress in urban tunnels have typically been set as low as 3–7 l/min per 100 m tunnel. This has resulted in a need for more extensive PEG, typically requiring 30 to 70 grouting holes per round, for tunnel cross sections varying from 65 to 113 $m^2$.

This paper compiles monitoring data from Norwegian tunnels, mainly in the Oslo region, constructed during the last 20 years with the existing Norwegian tunnel database from Karlsrud et al. (2003). In total, this extensive database covers 44 tunnels constructed over 45 years in Norway. The main problem addressed in this paper is the water ingress to tunnels resulting in pore pressure reduction, which can cause settlements in overlying soft soil deposits. The complex cross-disciplinary nature of this problem requires the integration of skillsets covering engineering geology, hydrogeology and geotechnical engineering. This poses a challenge in the complete understanding of the governing parameters, and consequently the difficulty of reducing the risk for settlements. The main aim of this paper is to highlight key trends and relations between parameters commonly monitored in tunnelling projects, such as water ingress, pore pressure reduction and grouting effort. This will provide a basis for the planning and construction of future tunnel projects. Furthermore, based on the analysis of the data, improved methods for monitoring and assessment of the performance of PEG during construction are suggested, to achieve watertightness needed in future tunnel projects.

## 2. Typical rock and soil conditions in the Oslo region, and sensitivity to pore pressure reduction

The geological conditions in the Oslo region consist of bedrock dating from the Precambrian, Cambro-Silurian, and Carboniferous and Permian periods. A graben structure was created by the Caledonian folding and Permian block faulting, resulting in the following main rock types:

- Igneous rocks (including both plutonic and volcanic) - Carboniferous and Permian
- Shale and limestone (sedimentary rocks) - Cambro-Silurian
- Gneiss - Precambrian

A bedrock map of the Oslo region is shown in Fig. 3 (based on Bjørlykke, 2004). The lower-lying areas of the city centre and nearby regions consist mainly of Cambro-Silurian sedimentary rocks such as shale and limestone. Igneous dikes (mostly syenite-porphyry and diabase) are common in these formations with thicknesses ranging from around half a meter to 50 m. The main igneous rocks in the Oslo region are syenite/monzonite, granite and rhombus porphyry, which makes up the hills and ridges to the north and west of the city centre. Precambrian gneissic rocks dominate the areas south and southeast of the city centre.

Research has shown that igneous rocks are often more brittle and tend to have more open channels along the joints compared to other rock types (Klüver, 2000). As an example, in the Oslo region it has been documented that syenite (plutonic) and Permian dikes, such as syenite porphyry and diabase, have higher hydraulic conductivity than other rock types (Holmøy, 2008, and Lindstrøm and Kveen, 2005).

The soil deposits above the bedrock typically consist of soft marine clays (0–80 m thick) deposited at the end of the last glaciation, about 10,000 years ago. These clays have not been subjected to loads greater than the present overburden stress and are normally consolidated (Bjerrum, 1967), with an apparent over-consolidation ratio (OCR, the ratio between the pre-consolidation stress and the in-situ effective overburden stress) of 1.2–1.4 due to ageing (Bjerrum, 1973). Commonly there is a layer of glacial moraine between the bedrock surface and overlying marine clay. This layer exhibits significantly higher hydraulic conductivity than the clay deposit, and hence represents a permeable aquifer which extends along the bedrock surface. Pore pressure levels in such confined aquifers are sensitive to changes in water infiltration and extraction, such as water ingress to tunnels.

To illustrate the nature of time-dependant settlements, Fig. 3 shows an example of calculated pore pressure reduction of 100 kPa at bedrock

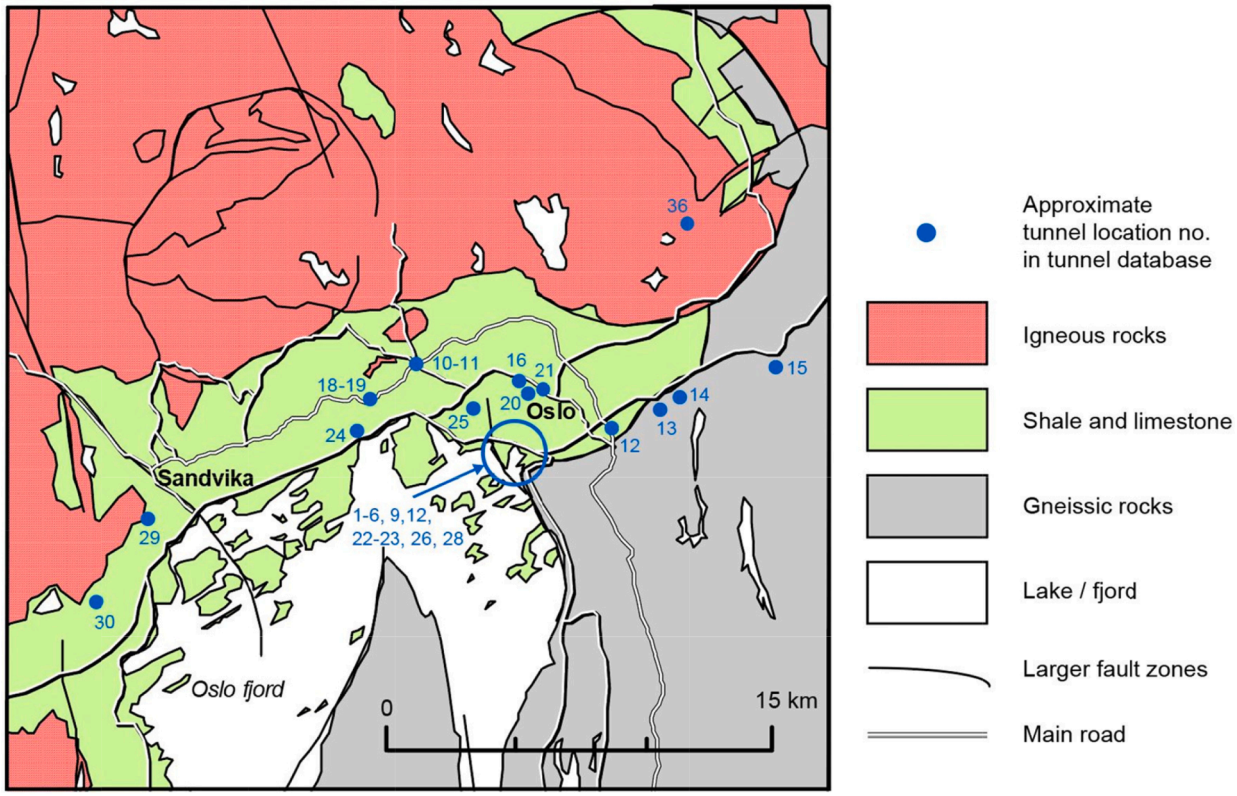


**Fig. 3.** Location of the tunnels in the Oslo region in the database. Bedrock map modified from Bjørlykke (2004).

level under a 20 m thick clay deposit, with OCR = 1.2. The calculations are performed using the Janbu modulus concept (Janbu, 1970), widely used in the Nordic countries to calculate consolidation settlements in clay (Andresen & Jostad, 2004). As the OCR is close to 1, minor changes in effective stresses, i.e., reduction in pore pressure, will cause significant consolidation settlements. The hydraulic conductivity of the clay is

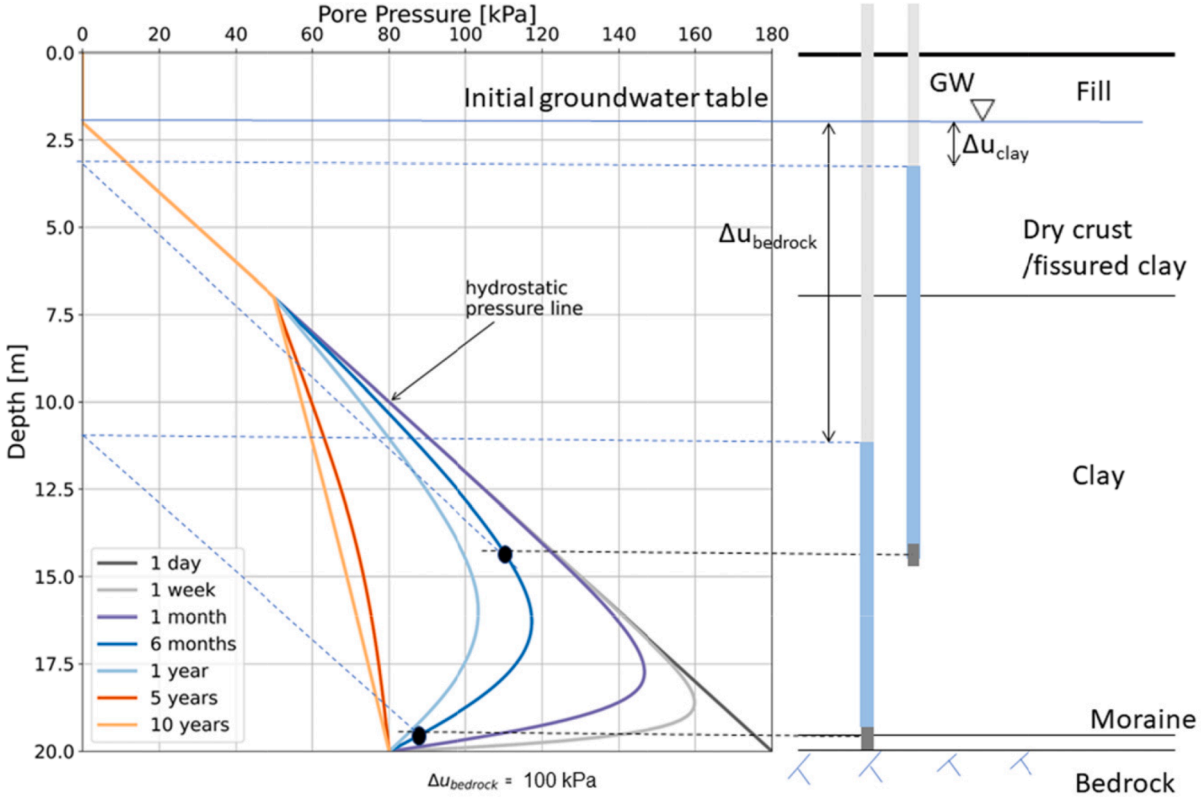


**Fig. 4.** Example of calculated pore pressure profiles with time in a clay profile.

set to $5{\cdot}10^{-10}$ m/s. The pore pressure reduction in the clay deposit is calculated for different time intervals. The low hydraulic conductivity of the clay layer results in a long consolidation process. From Fig. 4 it is apparent that the pore pressures need to be monitored at the bedrock surface to detect any effects of water ingress to tunnels. In the example it will take more than 6 months for pore pressures at 10 m depth to be affected. For the case at hand, the corresponding settlement at ground surface will be over 10 cm, as shown in Fig. 5.

## 3. Norwegian tunnel database

The database contains data from 44 tunnel projects, mostly in the Oslo region, constructed between 1975 and 2020. The original database from Karlsrud et al. (2003) contained 29 tunnels. In this revision, data from 15 additional tunnels has been added, mostly from tunnels constructed after 2000. An overview of the complete database is given in Appendix A.

For some projects, data has been monitored in several sections along the tunnel, in other projects data has been monitored over the total tunnel length. In total, the database contains monitoring data from 56 sections. All tunnels have been excavated using drill and blast excavation technique. All sections have strict limits on water ingress, which has required extensive PEG. The locations of the tunnels in the Oslo region are shown in Fig. 3, together with the three main bedrock types. The extent and quality of geological mapping varies across projects. In some cases, jointing, rock type and weakness- or fault zones were not described in detail. This paper therefore focuses on assessing the data with respect to the main rock types in the Oslo region.

The following data are registered in the database:

- Type: railway, subway, road, sewage, or energy,
- Year finished: end of construction,
- Tunnel Length [m]: length of bedrock tunnel, or tunnel section,
- Bedrock type: SL - Shale and limestone, I - Igneous (syenite, granite/monzonite, rhombus-, syenite porphyry), G – Gneiss
- h [m]: average tunnel depth under groundwater table,
- $R_e$ [m]: calculated equivalent radius, based on cross-sectional area of the tunnel $r_e=\sqrt{(A/\pi)}$,
- $D_n$ [m/m$^2$/m]: drilling length for grouting holes normalized over cross-sectional area and tunnel length,
- $G_n$ [kg/m$^2$/m]: amount of grouting material normalized over cross-sectional area and tunnel length,

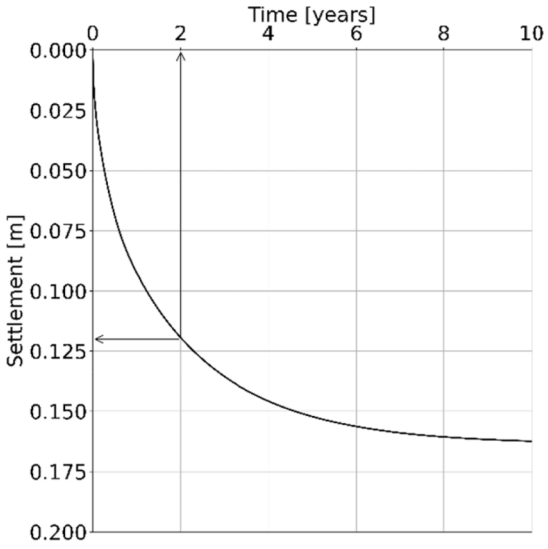


**Fig. 5.** Example of calculated settlement over time for 10 m pore pressure reduction as given in Fig. 3.

- q [l/min/100 m]: measured water ingress over concrete thresholds, given in litres per minute and 100 m tunnel length. The section length for the measurements varies from 150 m to several kilometres,
- $\Delta u_F$ [m]: measured pore pressure reduction in piezometers installed at bedrock level, in interface between bedrock and clay, or in moraine layer overlying the bedrock,
- Artificial water infiltration and infiltration amount [l/min]: some tunnels had water infiltration in bedrock wells, which affected the pore pressure reduction. The infiltration amount is the sum of infiltration flow in all installed wells,
- $k_i$ [m/s/m]: back-calculated hydraulic conductivity of the grouted zone assessed using the equation from NGI (1998) and Karlsrud (2000),

$$Q = \pi k_i h \frac{2}{ln\left(\frac{(R_e+t)}{R_e}\right)} \quad (1)$$

where Q = water ingress to tunnel after PEG [m$^3$/s/m].
$k_i$ = hydraulic conductivity of the grouted rock zone [m/s].
h = depth below the groundwater table [m].
$R_e$ = equivalent radius of the tunnel [m].
t = thickness of the grouted zone [m], assumed at 10 m for traffic tunnels and 5 m for sewage tunnels.

Several equations may be used for back-calculating the hydraulic conductivity (El Tani, 2003, and Park et al., 2008). The equation given by Karlsrud et al. (2003) is used for back-calculation of the hydraulic conductivity in this paper, consistent with previous publications for tunnel projects in Norway. Karlsrud's equation has been shown to overestimate the water inflow rate for shallow tunnels with ratios of $R_e$ /h $< 0.5$ to 1.0 (El Tani, 2003). In the database, the tunnel depth below the groundwater table is more than twice the tunnel radius for all tunnel sections, with two exceptions. Hence, the approximation is considered sufficiently valid for this study.

The data has been provided by the clients and consultants involved in the planning and execution of the projects. The extent of the monitoring and quality of the monitoring varies between projects. Since the data is collected from completed projects, it has not been possible to influence the extent of monitoring. The data collected is considered representative of the Norwegian state-of-practice for monitoring of tunnelling projects in urban areas. A summary of the database is presented in Fig. 6.

## 4. Data analysis

### 4.1. Pore pressure reduction versus horizontal distance from tunnel

Pore pressure reduction at bedrock level has been recorded in 14 tunnel projects. Fig. 7 presents the measured decrease in pore pressure, in relation to horizontal distance from the tunnel centre. In a large number of projects pore pressure reduction has been observed up to several hundred of metres from the tunnel centreline, typically up to 400 m. This large spatial influence is due to hydrogeological conditions with a confined aquifer over bedrock, which is sensitive to drainage. In the right hand side of the figure the data is systemized with respect to the main bedrock type for the tunnels. There is no indication of a correlation between the magnitude of pore pressure reduction and bedrock type. One likely explanation for this is that the pore pressure response is primarily governed by the hydrogeological conditions of the confined aquifer underneath the clay, such as the orientation, areal extent, hydraulic conductivity and natural groundwater recharge. The scatter in data can also be explained by varying amounts of water ingress to the tunnels, as well as duration of the leakage to the tunnels with respect to time of monitoring. Despite the scatter, the data clearly highlight the potential for large reductions in pore pressure at significant distances from the tunnel centre line.

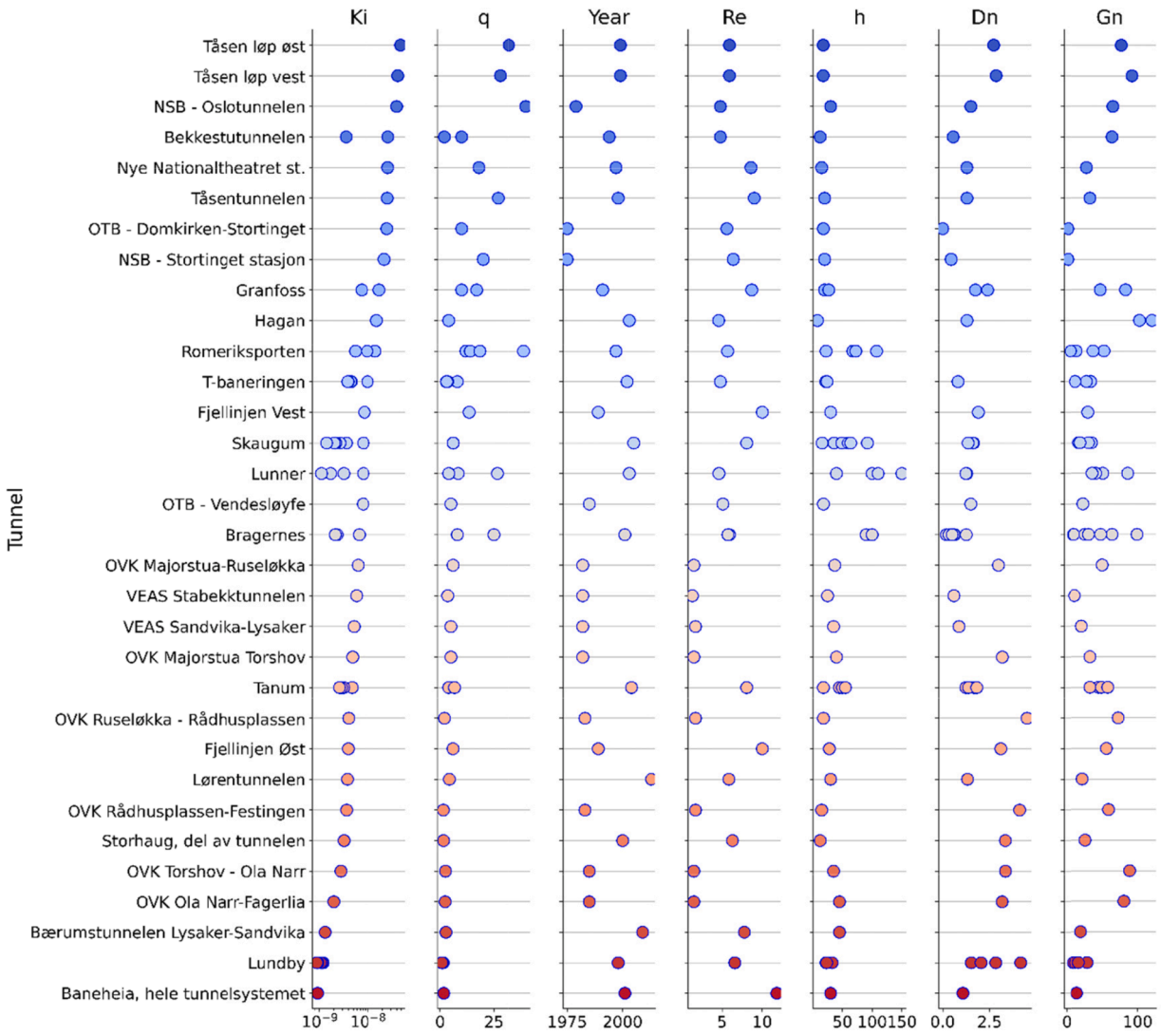


**Fig. 6.** Overview of some of the main data from the tunnel database, explanation to all parameters is given in the preceding section.

### *4.2. Water ingress versus pore pressure reduction*

Fig. 8 presents the measured decrease in pore pressure at bedrock along the centre line above the tunnel versus measured water ingress to the tunnel. This figure is used by the Norwegian tunneling industry to determine water ingress limits in urban areas. Based on acceptance criteria for settlements, the corresponding pore pressure reduction for areas overlying the tunnel is determined. The figure is then used to choose the water ingress limit. Normally, a pore pressure reduction of maximum 10–30 kPa will result in small settlements in a clay deposit with an apparent OCR of 1.2 to 1.4 due to ageing. The shaded area indicates values "normally accepted" suggested by Karlsrud et al. (2003), with q in the order of 3 to 7 l/min/100 m, i.e. flow rates expected to result in $\Delta u_F < 30$ kPa and normally chosen as a water limit design value. It is important to note that in areas with existing tunnels or other underground structures, the pore pressures may already have been affected by leakage, causing an increase in effective stress level and a corresponding decrease in apparent OCR of the marine clay. Any additional pore pressure decrease will cause additional consolidation settlements. In these areas, limits on water ingress may be even stricter than indicated in Fig. 8, down to 1–3 l/min/100 m.

Fig. 8 data from seven new tunnel projects have been added to the existing database. The points indicate the average monitored values, the grey crosses show the range of measured pore pressure reduction and inflow rates for each tunnel. Red data points show projects without artificial water infiltration. Blue datapoints show projects with artificial groundwater infiltration in bedrock wells. For these cases, the water is infiltrated at a constant rate in drilled bedrock holes, with packers installed at approximately 5 m depth into the bedrock. The infiltration will recharge the confined aquifer through fractures the bedrock and contribute to maintaining pore pressure levels. For these projects, the decrease in pore pressure is expected to be lower for a given water ingress, compared to projects without water infiltration.

Fig. 8 shows a considerable scatter in measured pore pressure reduction in relation to water ingress. This is likely caused by varying hydrogeological conditions previously described. In addition, there are uncertainties in the water ingress measurements, which are well-known to be challenging to perform. Furthermore, the length of the sections for

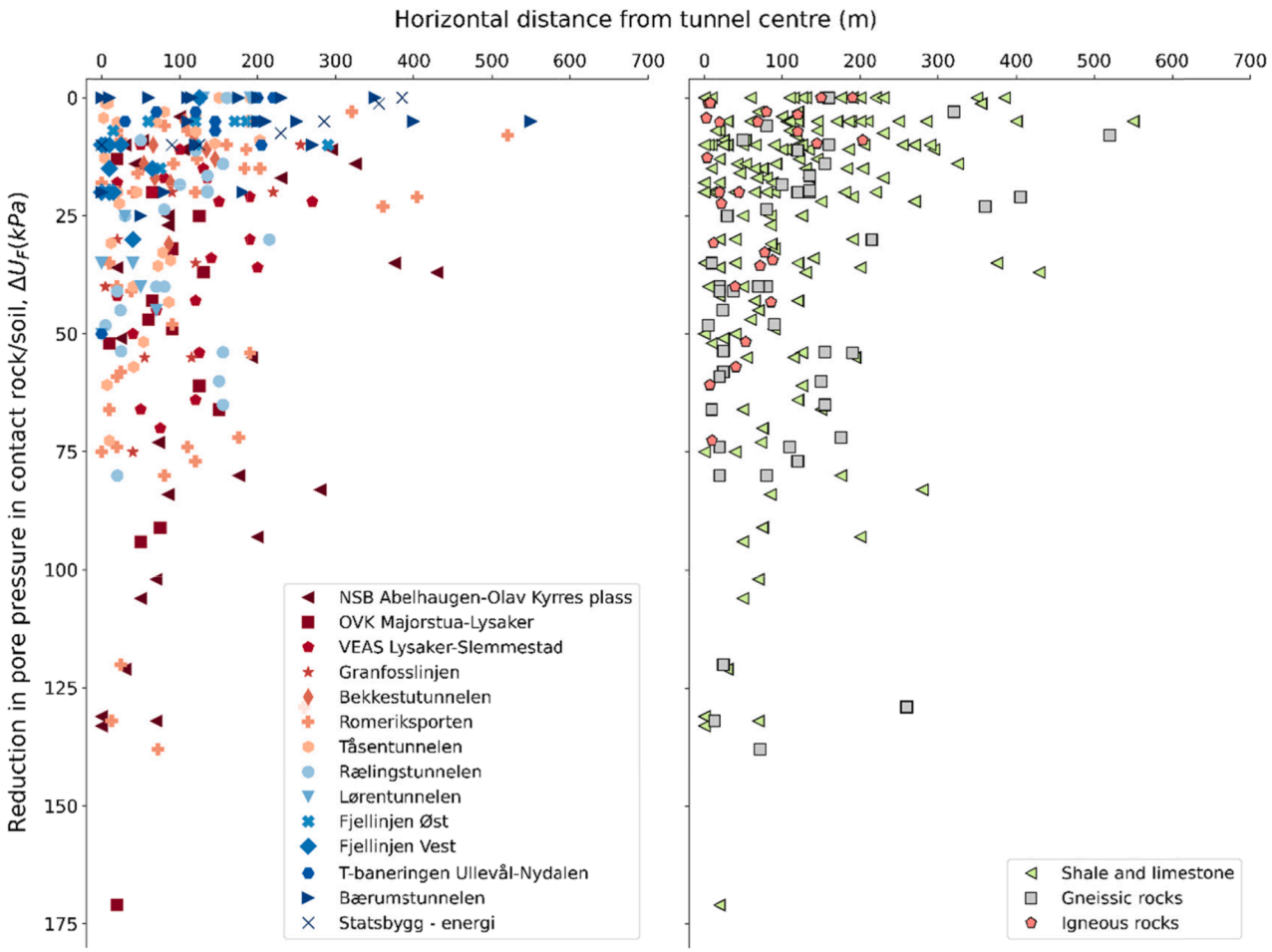


**Fig. 7.** Relationship between measured pore pressure reduction at soil/bedrock interface in relation to horizontal distance from tunnel centre line. In the left hand figure data is plotted for individual tunnels, in the right hand figure data is systemized with respect to main rock type (revised after Karlsrud et al., 2003).

water ingress measurements varies from 150 m to several kilometers. However, the water ingress, and resulting pore pressure reduction, can be concentrated around individual fault zones. Therefore, the accuracy of the individual measurements will vary, which contributes to additional uncertainty in the magnitude of the resulting pore pressure decrease for a given leakage rate. Nonetheless, there is a trend showing that pore pressure reduction increases with increasing water ingress. Based on the dataset a regression line has been derived for projects without water infiltration. This line is consistent with typical trendline previously suggested by Karlsrud et al. (2003). "Upper" and "lower" bound lines from Karlsrud et al. (2003) are shown in Fig. 8. These indicate a characteristic area for the $\Delta u_F$ to be expected, suggested in planning and design of tunnelling projects. The data from more recent tunnels (no. 19–26) are largely in agreement with previous data. Projects with water infiltration were excluded when deriving these lines, as they are affected by artificial recharge.

Many of the projects in the database were unable to meet the recommended water ingress limit of 3–7 l/min/100 m. However, all the case studies executed after 2002 (no. 20, 21, 24 and 26) have documented water ingress<7 l/min/100 m. This is an indication that more rigorous use of PEG, due to strict water ingress limits, can limit pore pressure reduction and settlements. The tunnel "NSB-National.-Skøyen" (no. 25) has the lowest registered water ingress of 1 l/min/100 m, this has been achieved through extensive post-excavation grouting.

There are a limited number of cases in the database where water infiltration has been used. In the tunnels "Fjellinjen vest" (no. 22) and "Nye Nationaltheatret st." (No. 23), relatively large infiltration rates of around 100 l/min were used, and the infiltration has had a clear effect on limiting pore pressure reduction. For the "Tåsentunnel" (no. 16), the infiltration rate is unknown. It is believed that the infiltration rate was limited, as the pore pressure reduction recorded is large (50 kPa). Despite the relatively few available data points, results indicate that water infiltration with large capacity can be an effective method for limiting pore pressure reduction during tunnel excavation.

### 4.3. *Back-calculated hydraulic conductivity versus grouting effort*

Since the 1990s, it has been standard practice in Norway to use systematic PEG and high grouting pressures in urban tunnels with strict limits on water ingress. The adopted grouting methodology consisted of dense drillhole patterns with overlapping grout rounds. The total drilled length for grouting holes is therefore an important parameter, in addition to the amount of grout used. Therefore, PEG efforts for the projects in the database are documented in terms of both grout consumption and drilling length for PEG. The drilling length and grout consumption have been normalized with respect to the cross-sectional area of the tunnel

1: NSB - Stortinget stasjon (1975)
2: NSB - Arbiensgt. (1979)
3: NSB - Parkvn. (1979)
4: NSB - Gyldenløvesgt. (1979)
5: NSB - Frogner (1979)
6: NSB - Erling Skjalgsonsgt. (1979)
7: OVK Majorstua- Kirkeveien (1977)
8: OVK Lysaker-Majorstua (1982)
9: Fjellinjen Øst (1989)
10: Granfoss, Lysaker (1991)
11: Granfoss, Ullern (1991)
12: Romeriksporten, Bryn (1997)
13: Romeriksporten, Godlia (1997)
14: Romeriksporten, Hellerud (1997)
15: Romeriksporten, Ellingsrud (1997)
16: Tåsentunnelen (1998)
17: Rælingstunnelen (1997)
18: Bekkestutunnelen, Gjønnes (1994)
19: Bekkestutunnelen, Egne hjem (1994)
20: Lørentunnelen (2013)
21: T-baneringen Ullevål-Nydalen (2002)
22: Fjellinjen Vest (1989)
23: Nye Nationaltheatret st. (1997)
24: Bærumstunnelen Lysaker-Sandvika (2009)
25: NSB - Nat. - Skøyen (post grouting) (1979)
26: Statsbygg-energy (2020)

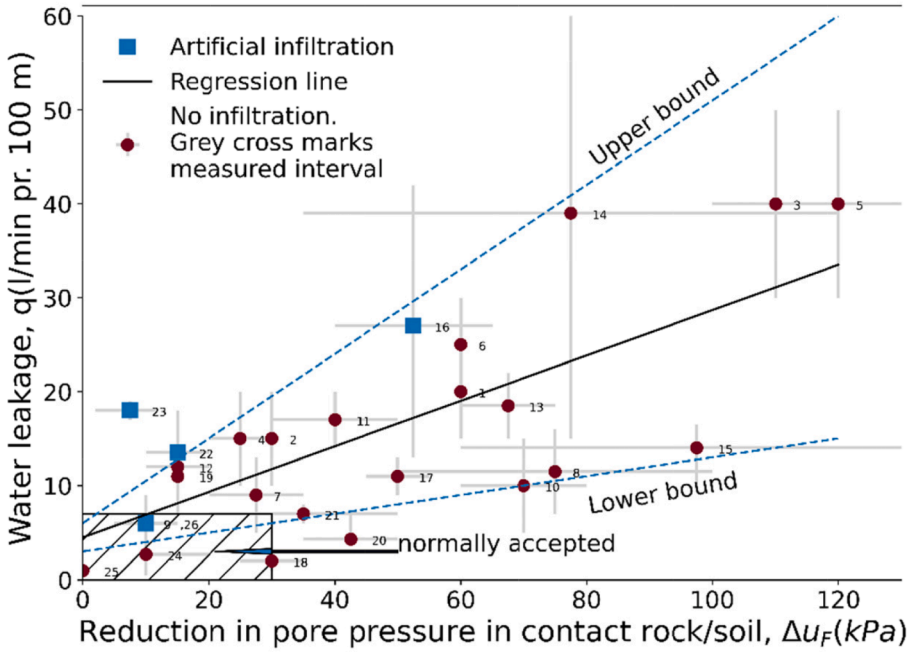


**Fig. 8.** Relationship between reduction in pore pressure at bedrock level and water ingress. Normally accepted area is indicated as shaded area (revised after Karlsrud et al., 2003).

and tunnel length, into a normalized drilling length, $D_n$, and normalized average grout consumption, $G_n$, as described in Section 2. For all tunnel sections the hydraulic conductivity of the grouted zone, $K_i$, is back-calculated according to Equation (1), using the average depth of the tunnel under the groundwater table, the measured water ingress and assumed thickness of the grouted zone (see Section 3).

In Fig. 9 and Fig. 10 the back-calculated $K_i$ is plotted in relation to $D_n$ and $G_n$. The figures give an indication of the total PEG effort undertaken. The data points are sorted according to main bedrock type, to assess if this has an influence on the grout effort and obtained $K_i$. The data in Fig. 9 and Fig. 10 shows significant scatter without clear correlations. A likely reason might be that $K_i$ is back-calculated from water ingress measurements over long sections, rather than measurements of leakage encountered in specific geological structures. Nevertheless, the figures imply that it is possible to obtain a hydraulic conductivity in the grouted zone of typically 4 to $6{\cdot}10^{-9}$ m/s, when applying standard Norwegian practice. The most watertight tunnels after PEG has a $K_i$ down to 1 to $2{\cdot}10^{-9}$ m/s.

Fig. 9 indicates that the drilling effort has been larger in shale and limestone tunnels, without obtaining a more water tight grouted zone. Experience from execution indicates that the shale and limestone formations require more grouting effort in terms of drilling for PEG, to achieve a certain water tightness compared with igneous rocks.

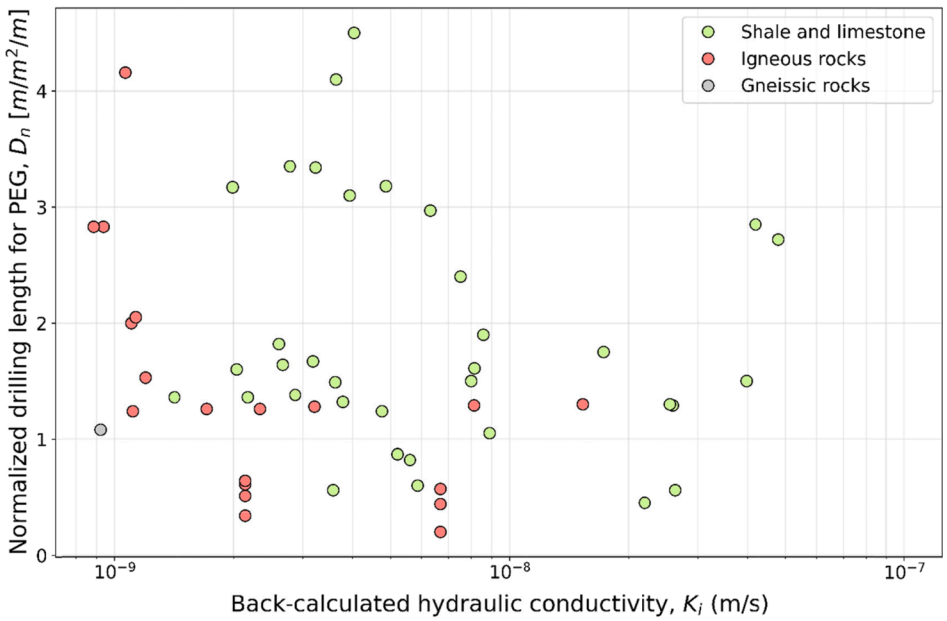


**Fig. 9.** Plot of back-calculated hydraulic conductivity of grouted zone in relation to drilling length for grouting (revised after Karlsrud et al., 2003).

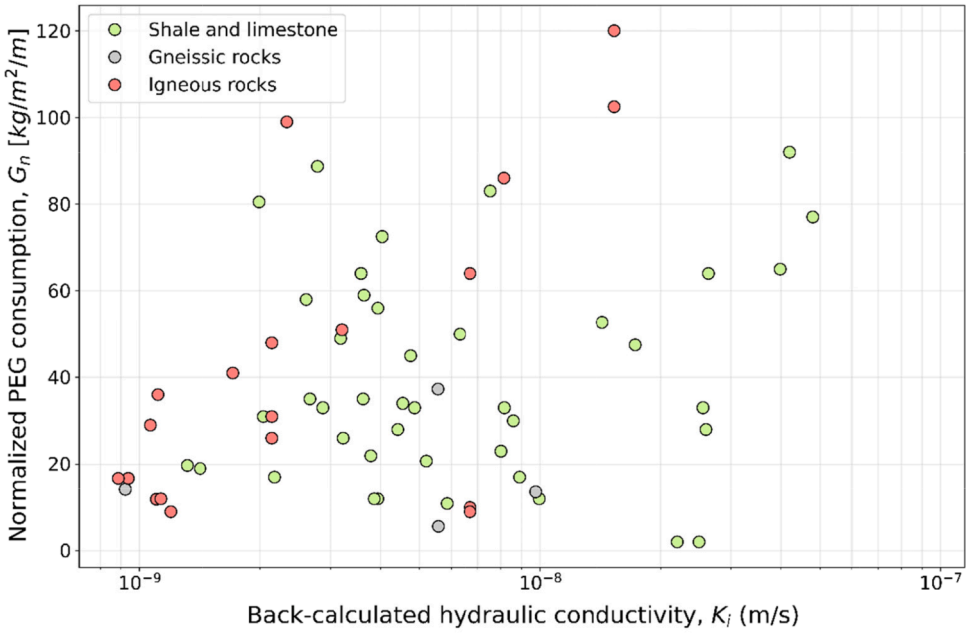


**Fig. 10.** Plot of back-calculated hydraulic conductivity of grouted zone in relation to grout consumption (revised after Karlsrud et al., 2003).

## 5. Discussion of results and implications for future tunnel projects

### *5.1. Uncertainty in the database and improved hydrogeological assessments*

Much of the scatter in the database may be related to challenges in measuring water ingress, resulting in variations and uncertainty in the data itself. In addition, the measurements are average rates taken over distances ranging from hundreds of meters to several kilometres, whereas it is well known that the water ingress is often concentrated around local fracture zones. Also, the data is strongly influenced by varying geological and hydrogeological conditions for each project, such as amount of natural groundwater recharge/infiltration which varies with topography, type of soil, size of catchment area for precipitation etc. Despite the scatter, the database provides unique insight into trends in terms of water ingress and pore pressure reduction and permits the suggestion of design limits for water ingress.

However, the data plotted in Fig. 8 imply that estimating pore pressure reduction from water ingress levels is related to significant uncertainty. Hence, monitoring of water ingress is an unsufficient measure to control pore pressure reduction. The resulting pore pressure reduction for a given leakage rate will vary depending on the hydrogeological conditions. An improved understanding of the sensitivity of pore pressure reduction in clay filled depressions could potentially be achieved with more detailed hydrogeological analysis. As an example, infiltration response tests (water loss measurements) can be performed during drilling of boreholes in bedrock for water infiltration wells. This requires installation of piezometers at bedrock level to monitor pressure levels during water infiltration. This type of test could be used to assess site-specific conditions, directly relating water infiltration rates to changes in pore pressure levels and allowing better understanding of the sensitivity of the areas to water ingress to tunnels.

### 5.2. Assessments of grouting performance and improved monitoring

Traditionally, water ingress measurements have been used for follow-up of PEG. One apparent issue with this is that monitoring of water ingress is undertaken after tunnel construction, and insight into whether limits have been met are registered after the tunnel is completed. The data presented in Fig. 7 shows that many projects projects have not complied with typical water ingress limits of 3–7 l/min/100 m. For future tunnels in urban areas already affected by subsurface development, limits on water ingress may be as low as 1–3 l/min/100 m (corresponding to small or no pore pressure reduction). This further emphasizes the need for pore pressure monitoring during construction, rather than monitoring of water ingress.

Challenges related to the uncertainty in water ingress measurements, and the importance of avoiding pore pressure reduction suggest that alternative monitoring methods are necessary. Monitoring of pore pressure at bedrock level during tunnel excavation can give early indications of unacceptable water ingress. Such monitoring can be carried out simultaneously with the PEG works, and hence can be used as criteria for assessing the result of the PEG during tunnel excavation. Furthermore, this approach can be used to adjust the details in the grouting methodology such as the number of drilling holes for grouting, the overlap between the grouting rounds, as well as the termination criteria for grouting pressure and grout amounts. Such an approach requires real-time monitoring of pore pressures during tunnel excavation. This is feasible with modern technology in monitoring and data processing, and is becoming a common practice in urban tunnelling projects in Norway. For the pore pressure data to be suitable for decision making during execution of PEG, one needs to distinguish the effects of the tunnelling from natural variations in pressure levels. One method which could be utilized is time series analysis, for example the open-source PASTAS script (Collenteur, 2019).

As stated, requirements on achieved watertightness will increase, as water ingress limits in future tunnel projects in urban enviroment likely will become stricter. To meet these requirements the PEG technology needs to be improved, with optimization of grouting fan layout and grout material properties. In addition, a direct method for assessing the hydraulic conductivity of the grouted zone is necessary. For this purpose more extensive use of water-loss measurements (Lugeon-measurements) after PEG can be utilized, to measure the effect of each grouting round and make necessary modifications to the PEG design.

### 5.3. Assessment of hydraulic conductivity and grouting effort with emphasis on main bedrock type

The data in Fig. 9 and Fig. 10 shows no correlations between PEG effort and main bedrock types. Nevertheless, Fig. 9 indicates that the drilling effort has been larger in shale and limestone tunnels, without

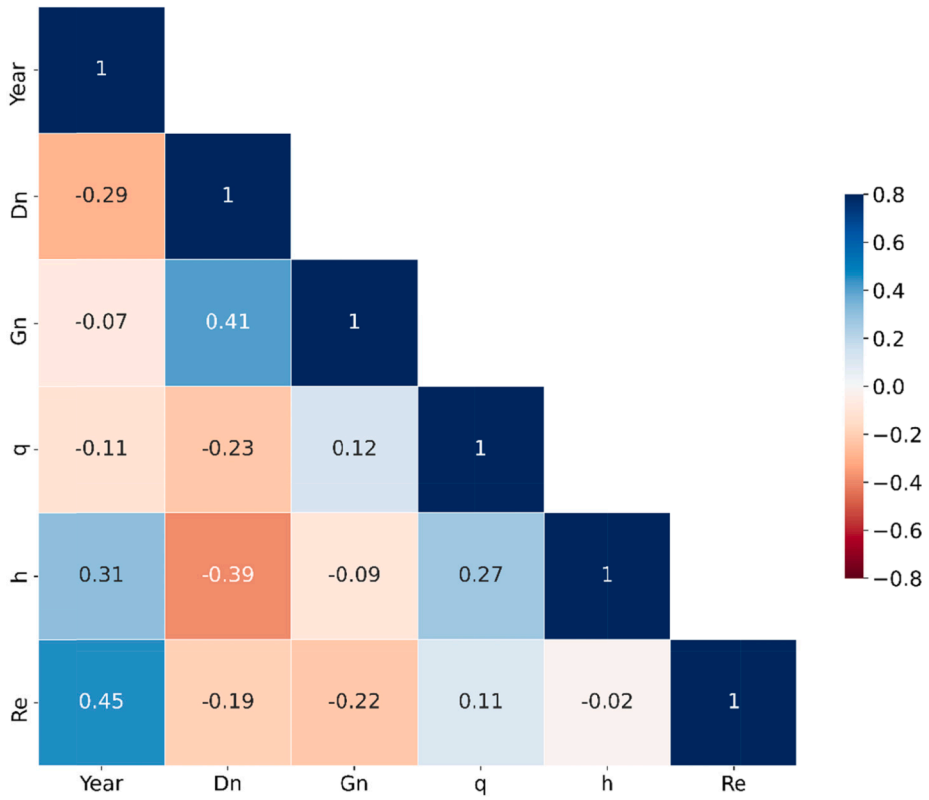


**Fig. 11.** Correlation matrix for parameters in database, using the Pearson correlation coefficient. 1 = max positive correlation, 0 = no correlation, −1 = max negative correlation.

obtaining a more watertight grouted zone. Experience from execution indicates that the shale and limestone formations require more grouting effort in terms of drilling for PEG, to achieve a certain water tightness compared with igneous rocks. This is consistent with Klüver's (2000) classification, where shale and limestone typically have lower hydraulic conductivity with discontinuous joints and clay-filled joints. Therefore, a larger number of grouting holes may be needed to intersect the transmissive joints and channels to achieve effective PEG.

The analyses herein with back-calculated hydraulic conductivity based on water ingress measurements over long sections, is not been detailed enough to find good correlations between pregrouting consumption and bedrock types. However, some of the tunnel projects included in the data base have been studied in more detail earlier (Holmøy, 2008, and Lindstrøm and Kveen, 2005). As an example, in the *T*-baneringen tunnel (Ullevål-Nydalen), a syenite porphyry dike, 15 m wide, caused high water ingress before PEG, compared to the rest of the tunnel. The syenite dike and nearby shale was highly jointed due to a fault zone, with Q-values between 0.01 and 0.3. The syenite porphyry dike gave higher water ingress than the rest of the tunnel, and after PEG the hydraulic conductivity was around $1{\cdot}10^{-8}$ m/s. The PEG consumption in syenite porphyry was higher than average, but the normalized drilling length was comparable to the surrounding rock mass. This is consistent with Klüver's (2000) rock mass classification, where syenite is typically representing a rock mass with open joints and high hydraulic conductivity and favourable for PEG, achieving the water tightness within a forecasted effort.

### 5.4. Correlation analysis

A correlation analysis (using the Pearson correlation coefficient) has been performed between tunnel-project specific properties, water ingress and grouting effort for projects in the database. The correlation matrix in Fig. 11 indicates a low correlation between pairs of variables in the dataset, with a few exceptions. This is not unusual for geological and hydrogeological problems, where correlation values of 0.3 to 0.5 can be considered to indicate medium to high correlations (Cesano et al., 2000, Henriksen, 2008; Holmøy, 2008). For the tunnel database no correlation values exceed 0.5, and only four of fifteen correlation values exceed 0.3. This indicates that water ingress is governed by many variables. In the following, only correlation values above 0.3 between pairs of variables will be discussed.

The positive correlation between $R_e$ (equivalent tunnel radius) and construction year, has its natural explanation in a tendency of increasing cross-sections for newer tunnels.

A positive correlation value of 0.41 is seen between drilling length and grouting volume. This result is not surprising, since increased drilling meters will give increased intersections of joints and penetration of grout material.

## 6. Conclusions

The presented Norwegian tunnel database is an extensive resource for planning, executing and monitoring of future tunnel projects in urban areas, to reduce the risk of unacceptable pore pressure reduction and consolidation settlements.

Based on the analysis of the data, the following statemens can be made:

- The additional recent data of water ingress and related pore pressure reduction (Fig. 8) are consistent with the database from Karlsrud et al. (2003). Pore pressure reduction is typically observed up to 400 m from the tunnel centre line (Fig. 7). The magnitude and the extent of pore pressure reduction is governed by hydrogeological conditions of the confined aquifer overlying the bedrock and not only the hydraulic conductivity of the rock mass.
- The large scatter in the data (Fig. 8) implies that it is necessary to focus on pore pressure monitoring in future projects, rather than water ingress, to reduce the risk of unacceptable pore pressure reduction.
- The data imply that it is possible to obtain a hydraulic conductivity in the grouted zone of typically 4 to $6{\cdot}10^{-9}$ m/s, when applying standard Norwegian practice. The most watertight tunnels after PEG has a $K_i$ down to 1 to $2{\cdot}10^{-9}$ m/s.
- The database gives indications of PEG effort, drilling for grouting holes (Fig. 9) and grout consumption (Fig. 10). However, there is no clear trend between back-calculated hydraulic conductivity in the grouted zone, $K_i$, and grouting effort, likely due to the uncertainties in water ingress measurements which is the basis for back-calculated $K_i$.

From the analyses it is apparent that focus should be aimed at monitoring pore pressure levels rather than water ingress, to reduce the risk of unacceptable pore pressure reduction and associated settlements. Real time monitoring of pore pressure during excavation and execution of PEG works, enables a more precise assessment of possible effects of tunnelling on pressure levels. This can aid decisions on necessary adjustments to PEG during construction. In addition, continued research and development of PEG technology is recommended to meet future stricter requirements on watertightness.

## CRediT authorship contribution statement

**Jenny Langford:** Conceptualization, Investigation, Validation, Writing – original draft, Project administration. **Kristin H. Holmøy:** Conceptualization, Investigation, Validation, Writing – original draft. **Tom Frode Hansen:** Formal analysis, Visualization. **Karl Gunnar Holter:** Writing – review & editing. **Eivind Stein:** Writing – review & editing.

## Declaration of Competing Interest

The authors declare that they have no known competing financial interests or personal relationships that could have appeared to influence the work reported in this paper.

## Data availability

The authors do not have permission to share data.

*Acknowledgements*

We would like to acknowledge the work carried out over years by our colleagues Kjell Karlsrud and Vidar Kveldsvik. A special thanks go to clients of the tunnel projects studied, and a special thanks to Statsbygg.

*Funding*

This research did not receive any specific grant from funding agencies in the public, commercial, or not-for-profit sectors.

## Appendix

| Case no | Tunnel | Type | Year finished | Tunnel length [km] | Bed-rock type | Depth under ground water level, h [m] | Equivalent radius, $R_e$ [m] | Drilling length, $D_n$ [m/m$^2$/m] | Amount of grouting material, $G_n$ [kg/m$^2$/m] | Water ingress q [l/min/100 m] | Pore pressure reduction over tunnel, at bedrock level $\Delta u_F$ [kPa] | Artificial water infiltration [l/min] | $K_i$ back-calc. (Karlsrud, 2000) [m/s] |
|---|---|---|---|---|---|---|---|---|---|---|---|---|---|
| 1* | NSB Stortinget stasjon | Subway | 1975 | 3.65 | SL | 18–22 | 6.4 | 0.45 | 2 | 15–25 | 60 | 0 | $2.2{\cdot}10^{-8}$ |
| 2* | NSB Arbiensgt. | Railway | 1979 | | SL | 30 | 4.8 | 1.5 | 65 | 10–20 | 30 | 0 | $3.98{\cdot}10^{-8}$ |
| 3* | NSB Parkvn. | Railway | 1979 | | SL | 30 | 4.8 | 1.5 | 65 | 20–40 | 100–120 | 0 | $3.98{\cdot}10^{-8}$ |
| 4* | NSB Gyldenl.gt | Railway | 1979 | | SL | 30 | 4.8 | 1.5 | 65 | 10–20 | 20–30 | 0 | $3.98{\cdot}10^{-8}$ |
| 5* | NSB Frogner | Railway | 1979 | | SL | 30 | 4.8 | 1.5 | 65 | 30–50 | 100–140 | 0 | $3.98{\cdot}10^{-8}$ |
| 6* | NSB Erling S.gt. | Railway | 1979 | | SL | 30 | 4.8 | 1.5 | 65 | 20–30 | 60 | 0 | $3.98{\cdot}10^{-8}$ |
| 7* | OVK Majorstua-Kirkeveien | Sewage | 1982 | 2.7 | SL | 40 | 1.5 | 2.97 | 50 | 5–13 | 20–35 | 0 | $6.3{\cdot}10^{-9}$ |
| 8* | OVK Lysaker-Majorstua | Sewage | 1982 | 1.4 | SL | 40 | 1.6 | | 33 | 7–16 | 50–100 | 0 | |
| 9* | Fjellinjen Øst | Road | 1989 | 0.75 | SL | 28 | 10 | 3.1 | 56 | 4–8 | 5–15 | 8 | $3.94{\cdot}10^{-9}$ |
| 10* | Granfoss. Lysaker | Road | 1991 | 0.9 | SL | 27 | 8.7 | 2.4 | 83 | 5–15 | 60–80 | 0 | $7.52{\cdot}10^{-9}$ |
| 11* | Granfoss. Ullern | Road | 1991 | 1.1 | SL | 20 | 8.7 | 1.75 | 47.5 | 14–20 | 30–50 | 0 | $1.73{\cdot}10^{-8}$ |
| 12* | Romeriksporten. Bryn | Railway | 1997 | 0.4 | SL | 23 | 5.7 | | 53 | 9–15 | 10–20 | 0 | $1.43{\cdot}10^{-8}$ |
| 13* | Romeriksporten. Godlia | Railway | 1997 | 1 | G | 73 | 5.7 | | 37 | 15–22 | 60–75 | 0 | $5.56{\cdot}10^{-9}$ |
| 14* | Romeriksporten. Hellerud | Railway | 1997 | 1 | G | 108 | 5.7 | | 14 | 15–62 | 35–120 | 0 | $9.76{\cdot}10^{-9}$ |
| 15* | Romeriksporten. Ellingsrud | Railway | 1997 | 1.05 | G | 68 | 5.7 | | 6 | 10–17 | 60–135 | 0 | $5.57{\cdot}10^{-9}$ |
| 16* | Tåsentunnelen | Road | 1998 | 0.95 | SL | 20 | 9 | 1.3–2.85 | 33–92 | 13–42 | 40–65 | unknown | $2.55–4.8{\cdot}10^{-8}$ |
| 17* | Rælingstunnelen | Road | 1997 | 1.8 | G | 18 | 8.7 | | | 9–13 | 45–55 | 0 | $1.85{\cdot}10^{-8}$ |
| 18* | Bekkestutunnelen. Gjønnes | Road | 1994 | 0.7 | SL | 12 | 4.8 | 0.56 | 64 | 1–2 | 5–35 | 0 | $3.58{\cdot}10^{-9}$ |
| 19* | Bekkestutunnelen. Egne hjem | Road | 1994 | 0.7 | SL | 12 | 4.8 | 0.56 | 64 | 7–14 | 10–20 | 0 | $2.63{\cdot}10^{-8}$ |
| 20 | Lørentunnelen | Road | 2013 | 0.91 | SL | 30 | 5.9 | 1.32 | 22 | 3.5–7 | 35–50 | 0 | $3.79{\cdot}10^{-9}$ |
| 21 | *T*-baneringen. Ullevål-Nydalen | Subway | 2002 | 1.2 | SL | 23 | 4.8 | 2.1 | 67 | 3–8 | 5–50 | 0 | $4{\cdot}10^{-9}$-$1{\cdot}10^{-8}$ |
| 22 | Fjellinjen Vest | Road | 1989 | 0.77 | SL | 30 | 10 | 1.9 | 30 | 11–18 | 10–20 | 100 | $8.58{\cdot}10^{-9}$ |
| 23 | Nye Nationalth. st. | Railway | 1997 | 0.27 | SL | 15 | 8.6 | 1.29 | 28 | 17–19 | 2–12 | 100 | $2.59{\cdot}10^{-8}$ |
| 24 | Bærumstunnelen Lysaker-Sandvika | Railway | 2009 | 7.8 | SL | 45 | 7.8 | | 20 | 0.5–9 | 0–20 | 0 | $1.32{\cdot}10^{-9}$ |
| 25 | NSB Nasjonaltheatret-Skøyen (after post grouting) | Railway | 1979 | | SL | 30 | 4.8 | | | 1 | | 0 | |
| 26 | Statsbygg | Energy | 2020 | UO | SL / G | UO | UO | 1.05 | 17 | 4–8 | 15 | 0 | $8.9{\cdot}10^{-9}$ |
| 27* | OTB Vendesløyfe | Railway | 1985 | | SL | 18 | 5.1 | 1.5 | 23 | 5 | | 0 | $8{\cdot}10^{-9}$ |
| 28* | OTB Sentrum stasjon | Railway | 1985 | | SL | 18 | 5.6 | | 2 | 10 | | 0 | $2.49{\cdot}10^{-8}$ |
| 29 | Tanum | Railway | 2004 | | SL | 50 | 8.1 | 1.2–1.8 | 33–58 | 7 | | 0 | $2{\cdot}5{\cdot}10^{-9}$ |
| 30 | Skaugum | Railway | 2005 | | SL | 70 | 8.1 | 1.3–1.6 | 17–35 | 6 | | 0 | $1{\cdot}8{\cdot}10^{-9}$ |
| 31 | Bragernes | Road | 2001 | 2.3 | I | 100 | 5.7 | 0.4–0.6 | 30–100 | 8–25 | | 0 | $2{\cdot}7{\cdot}10^{-9}$ |
| 32 | Lunner | Road | 2003 | 1.6 | I | 90 | 4.6 | 1.26 | 41 | 8 | | 0 | $2.9{\cdot}10^{-9}$ |
| 33 | Lundby (Swedish) | Road | 1998 | | I | 10–30 | 4.6 | 1.5–4 | 9 | 1 | | 0 | $1.1{\cdot}10^{-9}$ |
| 34 | Baneheia | Road | 2001 | | G | 30 | 11.8 | 1.1 | 14.2 | 2 | | 0 | $1{\cdot}10^{-9}$ |
| 35 | Storhaug | Road | 2000 | | SL | 12 | 6.2 | 3.34 | 26 | 1.6 | | 0 | $3.2{\cdot}10^{-9}$ |
| 36 | Hagan | Road | 2003 | | I | 8 | 4.63 | 1.3 | 102 | 4 | | 0 | $1.53{\cdot}10^{-8}$ |
| 37* | OVK Majorstua-Torshov | Sewage | 1982 | 3 | SL | 40 | 1.5 | 3.18 | 33 | 5 | | 0 | $4.86{\cdot}10^{-9}$ |
| 38* | OVK Majorstua-Ruseløkka | Sewage | 1982 | 2.7 | SL | 37 | 1.5 | 2.97 | 50 | 6 | | 0 | $6.31{\cdot}10^{-9}$ |
| 39* | OVK Torshov – Ola Narr | Sewage | 1985 | 1.7 | SL | 35 | 1.5 | 3.35 | 89 | 2.5 | | 0 | $2.78{\cdot}10^{-9}$ |
| 40* | OVK Ola Narr-Fagerlia | Sewage | 1985 | 2.4 | SL | 45 | 1.5 | 3.17 | 81 | 2.3 | | 0 | $1.99{\cdot}10^{-9}$ |
| 41* | OVK Ruseløkka-Rådhusplassen | Sewage | 1983 | 0.9 | SL | 18 | 1.7 | 4.5 | 73 | 2 | | 0 | $4.04{\cdot}10^{-9}$ |
| 42* | OVK Rådhusplassen-Festningen | Sewage | 1983 | 0.6 | SL | 15 | 1.7 | 4.1 | 59 | 1.5 | | 0 | $3.64{\cdot}10^{-9}$ |
| 43* | VEAS Sandvika-Lysaker | Sewage | 1982 | 10.5 | SL | 35 | 1.7 | 0.87 | 21 | 5 | | 0 | $5.20{\cdot}10^{-9}$ |
| 44* | VEAS Stabekktunnelen | Sewage | 1982 | 8.2 | SL | 25 | 1.3 | 0.6 | 11 | 3.5 | | 0 | $5.86{\cdot}10^{-9}$ |

* Published in Karlsrud et al., 2003, SL: Shale and limestone, I: Igneous, G: Gneiss.

## References


Abidin, H.Z., Andreas, H., Gumilar, I., Fukuda, Y., Pohan, Y.E., Deguchi, T., 2011. Land subsidence of Jakarta (Indonesia) and its relation with urban development. Nat. Hazards 59 (3), 1753–1771.

Andresen, L., Jostad, H.P., 2004: Janbu's Modulus Concept vs. Plaxis Soft Soil Model. Nordic Geotechnical Meeting NGM 2004 – XIV.

Barton, N., Quadros, E., 2019. Understanding the need for pre-injection from permeability measurements: What is the connection? J. Rock Mech. Geotech. Eng. 11 (3), 576–597.

Beitnes, A., 2002. Lessons to be learned from long railway tunnels. Water control in Norwegian tunnelling. Publication No. 12. Norwegian tunnelling society, 51-57.

Bjerrum, L., 1967. Engineering geology of Norwegian normally consolidated marine clays as related to settlements of buildings. 7th Rankine lecture. Géotechnique 17, 81–118.

Bjerrum, L., 1973. Problems of soil mechanical and construction on soft clays. State of the art report to Session IV. In: 8th International conference on soil mechanics and foundation engineering. Moscow, pp. 1–53.

Bjørlykke, K., 2004. Geology – The Oslo area. An over-view of the geology. University of Oslo.

Burbey, T.J., 2002: The influence of faults in baisin-filled deposits on land subsidence. Las Vegas Valley. Nevada. USA. Hydrogeology J. 10 (5), 525–538.

Cesano, D., Olofsson, B., Bagtzoglou, A.C., 2000. Parameters regulating groundwater inflows into hard rock tunnels - a statistical study of the Bolmen tunnel in southern Sweden. Tunn. Undergr. Space Technol. 15 (2), 153–165.

Collenteur, R.A., Bakker, M., Caljé, R., Klop, S.A., Schaars, F., 2019. Pastas. Open Source Software for the Analysis of Groundwater Time Series. Groundwater 57 (6), 877–885.

El Tani, M., 2003. Circular tunnel in a semi-infinite aquifer. Tunn. Undergr. Space Technol. 18 (1), 49–55.

Garshol, K.F., Tam, J.K.W., Mui, S.W.B., Chau, H.K.M., Lau, K.C.K., 2012. Grouting Techniques for Deep Subsea Sewage Tunnels in Hong Kong. World Tunnel Congress 2012. Bangkok, Thailand Underground and Tunnelling Group (TUTG).

Garshol, K.F., Tam J.K.W., Chau, H.K.M., Lau, K.C.K., 2014. Excavation of Dry Subsea Rock Tunnels in Hong Kong using Micro-Fine Cement and Colloidal Silica for Groundwater Control. Proceedings of the World Tunnel Congress 2014 – Tunnels for a better Life. Foz do Iguaçu, Brazil.

Henriksen, H., 2008. Late Quaternary regional geodynamics and hydraulic properties of the crystalline rocks of Fennoscandia. J. Geodyn. 45 (1), 49–62.

Holmøy, K.H., 2008. Significance of geological parameters for predicting water leakage in hard rock tunnels. Norwegian University of Science and Technology. Dissertation.

Holmsen, G., 1953. Regional settlements caused by a subway tunnel in Oslo. 3rd Int. Conf. Soil Mech. and Found. Eng. Proceedings. 1, 381–383.

Janbu, N., 1970. Soil mechanic – Basic Course. Norwegian University of Science and Technology. Trondheim, Tapir forlag. In Norwegian.

Karlsrud, K., Erikstad, L. Snilsberg, P., 2003: Investigations and water ingress limits for environmental friendly neighboorhood, Norwegian Public Roads Administration, Tunnels for the citizens, Report No. 103. In Norwegian.

Karlsrud, K., Vangelsten, B.V., 2017. Subsidence and land loss in the Ca Mau Province – Vietnam. Causes, consequences and mitigation options. Geotech. Eng. J. SEAGS & AGSSEA 48, No.1.

Karlsrud, K., 2000. Method for prediction of potential settlements and leakage limits in urban areas, Rock blasting conference. Oslo, pp. 24.1–24.19.

Klüver, B.H., 2000. Pregrouting in hard rock. Internal Report No. 2151, Norwegian Public Roads Administration. Oslo, 21 pp. In Norwegian.

Lindstrøm, M., Kveen, A., 2005. Tunnels for the citizen - Final Report. Norwegian Public Roads Administration. Tunnels for the citizens. Report No. 105. 62 pp. In Norwegian.

Myrabø, S., Moss-Iversen, E., 2014. The Romeriksporten tunnel. Tunnel-induced settlements – status report. Norwegian Tunnelling Society. Rock blasting conference, Oslo. pp. 20.1-20.10. In Norwegian.

Norwegian Geotechnical Institute (NGI), 1998. Water control in highly populated areas - data base. NGI Report No. 526521-1. Oslo, In Norwegian.

Norwegian Tunnelling Society (NTS), 1995. Urban tunnelling. Publication No. 10.

Norwegian Tunnelling Society (NTS), 2001. Water control. Publication No. 12.

Ortega-Guerrero, A., Rudolph, D.L., Cherry, J.A., 1999. Analysis of long-term land subsidence near Mexico City. Field investigations and predictive modelling. Water Resour. Res. 35 (11), 3327–3341.

Park, K.H., Owatsiriwong, A., Lee, J.G., 2008. Analytical solution for steady-state groundwater inflow into a drained circular tunnel in a semi-infinite aquifer: A revisit. Tunn. Undergr. Space Technol. 23, 206–209.

Pien-wej, N., Giao, P.H., Nutalaya, P., 2006. Landsubsidence in Bankgok Thailand. Eng. Geol. 82 (4), 187–201.

Shen, S.L., Wu, H.N., Cui, Y.J., Yin, Z.Y., 2014. Long-term settlement behaviour of metro tunnels in the soft deposits of Shanghai. Tunn. Undergr. Space Technol. 40, 309–323.

Xue, Y.Q., Zhang, Y., Ye, S.J., Wu, J.C., Li, Q.F., 2005. Land subsidence in China. Environ. Geol. 48 (6), 713–720.

Yoo, C., 2005. Interaction between tunnelling and groundwater - numerical investigation using three-dimensional stress-pore pressure coupled analysis. J. Geotech. Geoenviron. Eng., ASCE 131 (2), 240–250.

Yoo, C., Lee, Y., Kim, S.H., Kim, H.T., 2012. Tunnelling-induced ground settlements in a groundwater drawdown environment – A case history. Tunn. Undergr. Space Technol. 29, 69–77.

Zhu, L., Gong, H., Li, X., Wang, R., Chen, B., Dai, Z., Teatini, P., 2015. Land subsidence due to groundwater withdrawal in Northern Beijing Plain. China. Eng. Geol. 193, 243–255.